GEOPHYSICAL RESEARCH LETTERS, VOL. 35, L03619, doi:10.1029/2007GL032739, 2008

Effects of atmospheric vorticity on the seasonal hydrographic cycle over the eastern Siberian shelf

Igor A. Dmitrenko,[1] Sergey A. Kirillov,[2] L. B. Tremblay,[3] Dorothea Bauch,[1] and Mikhail Makhotin[2]

Received 20 November 2007; revised 4 January 2008; accepted 11 January 2008; published 14 February 2008.

[1] The seasonal hydrographic cycle explains about 25–75% of the entire salinity variability spectrum of the Siberian shelf hydrography. Quasi-decadal variations in the seasonal salinity difference over the Laptev and East Siberian sea shelves derived from continuous summer-to-winter historical records from the 1960s–1990s are attributed to atmospheric vorticity quasi-decadal variations. Summer cyclonic vorticity results in riverine water accumulation on the shelf, increasing the salinity summer-to-winter difference. Summer anticyclonic wind pattern enhances fresh water movement from the shelf towards the Arctic Ocean that tends to weaken the seasonal salinity amplitude.
Citation: Dmitrenko, I. A., S. A. Kirillov, L. B. Tremblay, D. Bauch, and M. Makhotin (2008), Effects of atmospheric vorticity on the seasonal hydrographic cycle over the eastern Siberian shelf, *Geophys. Res. Lett.*, *35*, L03619, doi:10.1029/2007GL032739.

1. Introduction

[2] The seasonal hydrographic cycle is forced by river runoff and ice melting during summer, and thermodynamic ice formation that provides a strong salt input through brine release during winter. Through these processes the seasonal hydrographic cycle modifies shelf water and maintains control on the Arctic Ocean cold halocline layer [*Aagaard et al.*, 1981; *Melling and Moore*, 1995; *Rudels et al.*, 1996]. The number of publications discussing seasonal hydrographic cycling over the Eurasian shelf is limited to several early Russian papers by *Shpaikher and Fedorova* [1977, 1978] mainly focused on seasonal heat content variability, and recent modeling by *Harms and Karcher* [1999], simulating the Kara Sea seasonal cycle of temperature, salinity and water circulation using climatological forcing. The present study for the first time addresses the issue of seasonal hydrographic cycling and its variability over the eastern Siberian shelf, consisting of the Laptev and East Siberian seas (Figure 1), using continuous summer-to-winter Soviet hydrographic observations from the 1960s–1990s.

2. Data

[3] Winter historical hydrographic data from 2839 stations were obtained during Soviet aircraft surveys from March to May in the 1960s–1990s. Summer ship-based observations (11360 stations) were collected in the ice-free regions of the Laptev and East Siberian seas in August–September 1920–2005 (see Figure 1 for spatial and temporal coverage). Prior to 1993, salinity was measured with a Russian GM-65 salinometer with an accuracy of 0.05 psu, while in recent years, data come from CTD measurements with a salinity accuracy of greater than 0.01 psu. The summer-to-winter hydrographic surveys cover the entire thirty-year period from 1963–1993. National Center for Environmental Prediction (NCEP) sea level pressure (SLP) data were employed to describe the atmospheric circulation over the Arctic Ocean. Monthly mean discharge of Siberian rivers was taken from Arctic-RIMS (Regional Integrated Monitoring System).

3. Methods

[4] For each summer and winter season the salinity snapshot measurements in the upper 70 m layer were linearly interpolated over a 120 km search radius onto a regular grid with horizontal and vertical resolution of 50 km and 1 m, respectively. The long-term mean depth-averaged summer-to-winter seasonal salinity difference (SSD) was computed at each node by averaging the winter and previous summer vertically-integrated salinity difference over the period of continuous summer-to-winter hydrographic observations (1963–1993, Figure 2, top). In Figure 2 (middle), we show the SSD standard deviation. In order to keep the summer-to-winter budget closed, all salt sources from the ocean including the sea-ice are considered. During winter we assume a one-and-a-half- meter thick layer of sea-ice with a constant salinity of 10 psu reflecting the average value for one-year sea-ice [*Pfirman et al.*, 1990; *Melling and Moore*, 1995]. As sea-ice forms it can exhibit a wide range of salinity, from 5 to 12 psu, but salinity decreases rapidly with age [*Untersteiner*, 1968; *Pfirman et al.*, 1990; *Melling and Moore*, 1995]. The SSD shown in Figure 2 (top) is not very sensitive to the particular assumption regarding sea ice thickness and salinity. However over the shallows and coastline in the southern Laptev Sea the choice of sea-ice salinity does affect the SSD, resulting in artificially negative SSD values (Figure 2, top) at a sea-ice salinity less than 10 psu. To quantify the relative contribution of seasonal salinity variability to the entire salinity variability, the ratio of the long-term mean summer-to-winter SSD and standard deviation from the entire summer-to-winter salinity data set for the period of 1963–1993 was computed at each grid node where data are present (Figure 2, bottom). The zero level indicates no seasonal salinity variation, while the 100% level corresponds to a pure seasonal signal with no long-term component.

[1] Leibniz Institute of Marine Sciences, University of Kiel, Kiel, Germany.
[2] Arctic and Antarctic Research Institute, St. Petersburg, Russia.
[3] Oceans and Atmosphere Sciences, McGill University, Montreal, Quebec, Canada.

0094-8276/08/2007GL032739$05.00

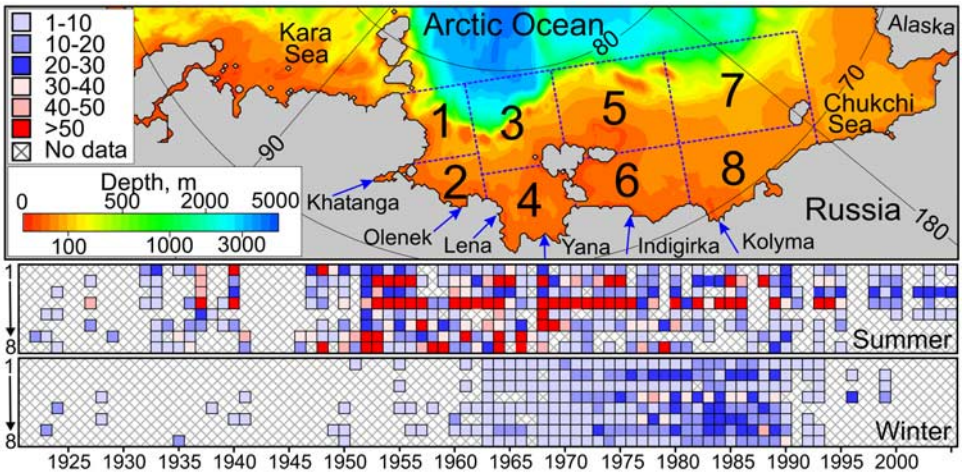

Figure 1. (top) Map of the eastern Arctic Ocean. Dashed lines show sub-regions of the Laptev (1–4) and East Siberian (5–8) seas. The number of stations occupied between 1920 and 2005 within sub-regions 1–8 is shown for (middle) summer and (bottom) winter. The color code is defined in the legend on the top-left corner of the Figure 1 (top). Rivers with runoff exceeding 20 km^3/summer are shown by the blue arrows.

[5] Time series of summer and winter yearly mean salinity for the Laptev and East Siberian seas were calculated by averaging the salinity field over both depth and surface area from 1961 to 1991. This approach was motivated by the fact that significant spatial variability in the long-term mean SSD was observed (Figure 2, top, and Figure 2, middle). The method used to integrate the salinity over a regular grid (x, y and z) follows that of *Dmitrenko et al.* [2007]. Differences in station locations and data spatial coverage from year to year significantly complicate the interpretation of salinity time series. A 7-year running mean was applied to the summer and winter salinity time series to filter the noise associated with the limited data coverage. The conclusions presented hereafter focus mainly on lower-frequency (5–10 years) variability and are insensitive to the exact number of years used in the running average. The resulting salinity time series for the period of continuous summer-to-winter observations composed of the 7-year running mean of summer and winter salinity time series are shown in Figure 3 (top) and Figure 3 (middle).

[6] We used a vorticity index as a descriptor of atmospheric circulation to analyze summer-to-winter salinity time series. The vorticity index (developed by *Walsh et al.* [1996]) shows the sign and intensity of atmospheric vorticity. It is defined as the numerator of the finite-difference Laplacian of SLP for an area within a 550 km radius (following *Walsh et al.* [1996]) around 85°N and 125°E, a region located in the Arctic Ocean close to the northeastern Laptev Sea. A negative vorticity index corresponds to anticyclonic, and a positive index to cyclonic regimes of atmospheric circulation. The time series of vorticity (Figure 3, bottom) was calculated from the 7-year running mean of summer (June–September) and winter (November–May) mean vorticity indices derived from monthly NCEP SLP data.

4. Results

[7] The seasonal salinity cycling explains approximately 25–60% of the entire salinity variability spectrum over the

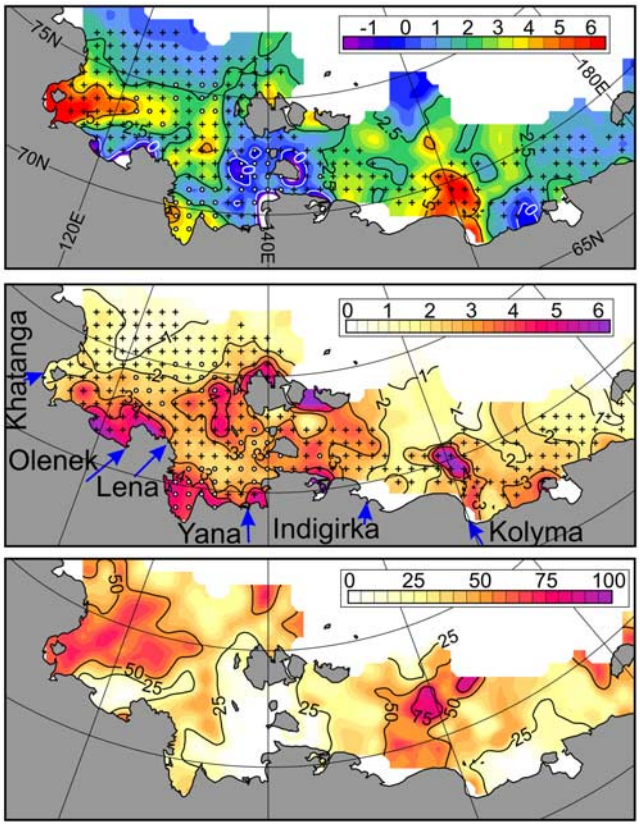

Figure 2. (top) The long-term mean (1960s–1990s) vertically-integrated summer-to-winter salinity difference (psu), and (middle) its standard deviation (psu). Dots mark those grid nodes where the salinity data from 15–30 years of continuous summer-to-winter observations were used. Crosses correspond to 5–15 years of continuous summer-to-winter observations. Grid nodes with fewer than 5 summer-to-winter observations are not depicted. (bottom) The relative contribution of the seasonal salinity variability to the entire salinity variability (see text for more detailed explanation).

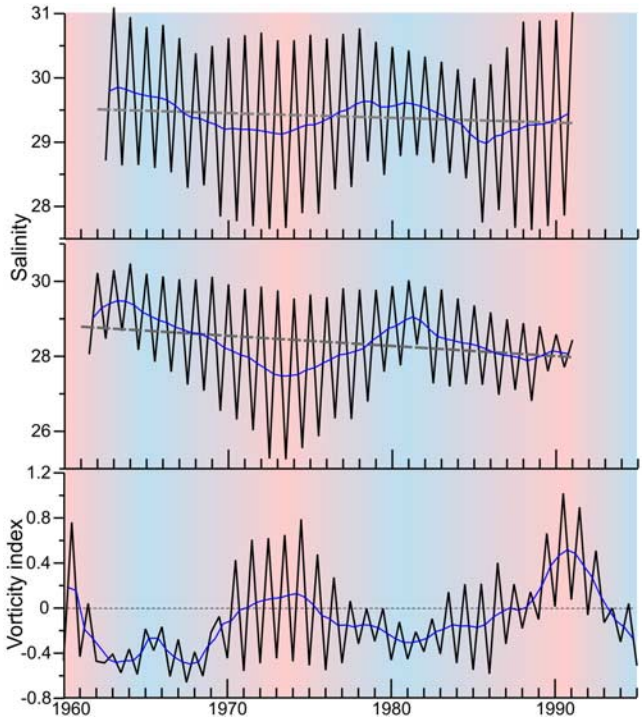

Figure 3. Time series of the mean salinity for the (top) Laptev and (middle) East Siberian seas. The linear trend is shown by dashed gray lines. (bottom) Seasonal mean atmospheric vorticity over an area within a 550 km radius around 85°N and 125°E. The blue curve is a 7-year running mean. Red and blue shading indicate positive (cyclonic) and negative (anticyclonic) summer vorticity periods, respectively.

eastern Siberian shelf (Figure 2, bottom), depending on the region. The seasonal component dominates the western Laptev Sea and the central East Siberian Sea where its contribution ranges from 50 to 75%. Over the southeastern Laptev and southwestern East Siberian seas, the seasonal cycling input is minimal and explains less than 25% of the total salinity variability. The SSD exhibits significant spatial variability with a maximal value of 4–6 psu in the western-central Laptev Sea and in the southern-central East Siberian Sea (Figure 2, top). The SSD standard deviation (Figure 2, middle) exceeds 3 psu (1) along the coastline in the southern Laptev Sea, (2) over the shallows adjoining the islands bordering the Laptev and the East Siberian seas, and (3) in the south-central East Siberian Sea.

[8] Unlike the SSD spatial distribution that exhibits no clearly attributable patterns, the summer-to-winter 7-year running mean time series (Figure 3, top, and Figure 3, middle) reveal characteristic features of seasonal hydrographic cycling. We calculate the long-term mean SSD to be 2.44 and 2.65 psu for the Laptev and East Siberian seas, with standard deviation of 0.49 and 0.98 psu, respectively. The quasi-decadal variability of the SSD is of particular interest. For the Laptev Sea the periods of 1963–1968 and 1978–1983 exhibit a relatively low mean SSD of 2.27 and 1.81, respectively. In contrast, the 1970–1976 and 1985–1991 periods demonstrate higher values of 2.80 and 2.83 (Figure 3, top). The time series for the East Siberian Sea (Figure 3, middle) demonstrates almost the same pattern with the exception of 1985–1991, when the seasonal salinity amplitude exhibits a tendency to decrease (compare 3.93 for 1970–1976 with 1.61 for 1985–1991).

5. Discussion

[9] The shallow Siberian shelf is believed to be sensitive to wind forcing. *Polyakov and Johnson* [2000], *Johnson and Polyakov* [2001], and *Steele and Ermold* [2004] all reported a relationship between decadal variability in sea surface salinity anomalies on the Siberian shelf and the Arctic Oscillation or North Atlantic Oscillation – two atmospheric circulation indices that are closely related to the extent to which storms penetrate into the eastern Arctic. From these considerations, *Dmitrenko et al.* [2005, 2007] reported that during summer the atmospheric circulation drives the interannual spatial variability in the surface water layer as well as in the entire shelf water column. In particular, when the vorticity of the atmosphere on the shelves is anticyclonic, winds typically exhibit off-shore (northward) components over the Laptev Sea and along-shore (westward) components over the East Siberian Sea shelf. As a result, approximately 500 km^3 of riverine fresh water migrates from the eastern Siberian shelf to the Arctic Ocean through the northeastern Laptev Sea. When the vorticity of the atmosphere is cyclonic, wind is oriented

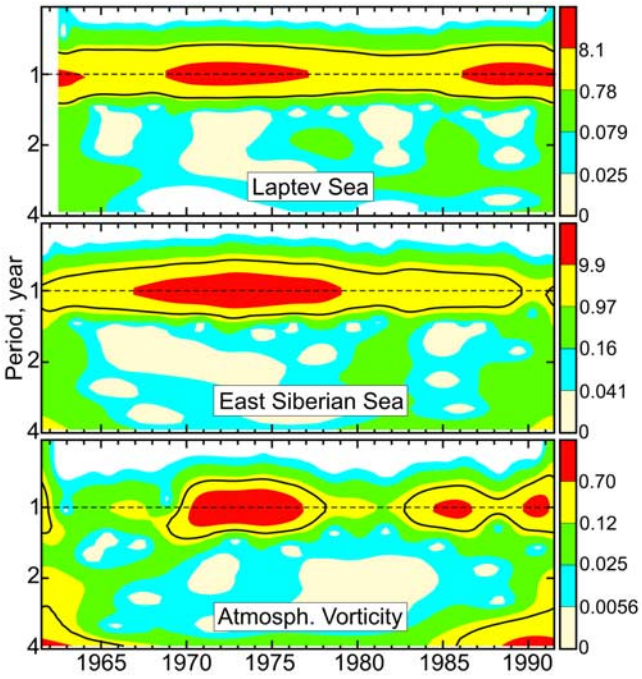

Figure 4. The wavelet power spectrum for the time series of (top, middle) salinity and (bottom) vorticity index shown in Figure 3 using the Morlet wavelet transform. The contour levels are chosen so that 75%, 50%, 25%, and 5% of the wavelet power is above each level indicated by red, yellow, green, and blue, respectively, in each of the three panels. The black contour lines show the 90% confidence level, using a white-noise background spectrum. The black dashed lines mark the one-year period associated with seasonal cycling.

along-shore towards the east over the entire Laptev Sea, and fresh water remains on the southern Laptev and East Siberian sea shelves [*Dmitrenko et al.*, 2005, 2007]. In contrast to the summer atmospheric circulation which is characterized by quasi-decadal oscillations between cyclonic and anticyclonic mode, the winter atmospheric circulation is relatively stable and anticyclonic with a weak relationship between winter atmospheric circulation and winter surface hydrography [*Dmitrenko et al.*, 2005].

[10] Our analysis demonstrates that the seasonal difference between predominantly cyclonic summers and anticyclonic winters is obvious (Figure 3, bottom). The vorticity index time series is dominated by strong seasonality with higher values during summer and lower values during winter (Figure 3, bottom). This feature is superimposed on quasi-decadal variability. Between 1962 and 1970, the vorticity demonstrates negative (anticyclonic) values for both winter and summer, but still maintains seasonality. Subsequently, until 1977, the seasonality becomes more pronounced with positive (cyclonic) values during summer and negative (anticyclonic) values during winter. The 1977–1982 period in general demonstrates almost the same patterns as those of 1962–1970. The first part of the 1983–1993 period exhibits the typical patterns of cyclonic summers and anticyclonic winters as in 1970–1977. After 1989, in contrast to 1970–1977, the winter vorticity index changes to more positive (cyclonic) values (Figure 3, bottom).

[11] We hypothesize that quasi-decadal shifts between cyclonic and anticyclonic summer wind patterns amplifies the seasonal hydrographic cycling over the eastern Siberian shelf. Summer cyclonic vorticity results in riverine water accumulation on the shelf [*Dmitrenko et al.*, 2007], increasing the SSD by 0.36–0.39 and 1.28 psu for the Laptev and East Siberian seas, respectively (Figure 3, top). In contrast to cyclonic vorticity, the anticyclonic wind pattern causes fresh water loss from the shelf to the Arctic Ocean during summer [*Dmitrenko et al.*, 2007]. This tends to decrease the SSD by 0.16–0.63 and 0.22–0.29 psu in the Laptev and East Siberian seas, respectively (Figure 3, top).

[12] The wavelet transform method allows the changing spectral composition of non-stationary signals to be measured and compared [*Foufoula-Georgiou and Kumar*, 1995]. The wavelet power spectra for the time series of salinity (Figure 4, top, and Figure 4, middle) and vorticity index (Figure 4, bottom) exhibit similar high-energy patterns (marked with red) at a seasonal frequency that are highly suggestive of a linkage between seasonal amplification of atmospheric vorticity and seasonal hydrographic cycling. For the Laptev Sea the periods with higher SSD from 1970–1976 and 1985–1991 (Figure 4, top) roughly coincide with quasi-decadal amplification of the atmospheric vorticity from 1970–1977, 1984–1988, and 1989–1992 (Figure 4, bottom). The East Siberian Sea exhibits the same regularity in 1970–1976, although from 1985–1991 we find an opposite tendency to a lower SSD while the seasonal amplitude of atmospheric vorticity tends to increase.

[13] More precise evidence of the relationship between seasonal salinity cycling and atmospheric circulation comes from the high correlation between the wavelet power spectra of atmospheric vorticity and salinity for the period of seasonal variability marked in Figure 4 with a dashed line. A statistically significant correlation of 0.64 and 0.68 for the Laptev and East Siberian seas, respectively, provides a qualitative assessment of seasonal hydrographic cycling amplification by atmospheric forcing.

[14] Figure 3 (middle) shows that the SSD anomaly in the East Siberian Sea was reduced from 1985–1991. This reduction does not adhere to the scenario described above; we attribute this departure from previous patterns to both a statistically significant negative winter salinity trend which started in 1981, and a statistically insignificant tendency for summer salinity to decrease that is likely associated with insufficient data coverage (Figure 1, bottom). We hypothesized that the observed winter freshening is likely due to less intensive ice production [*Rothrock and Zhang*, 2005] and diminished brine release. A clear attribution of East Siberian Sea winter freshening, without detailed consideration of ice-related processes and atmospheric winter vorticity state, however remains highly speculative.

[15] Interannual river discharge variability may be another potential contributor modifying seasonal hydrographic cycling. The Arctic-RIMS data show that about 40% of the mean annual Siberian river discharge takes place during river-ice breakup which usually occurs at the end of May and beginning of June. Between November and April steady low-flow discharge is observed. In fact, we have found no substantial correlation between time series of the summer-to-winter difference in seasonally-averaged river discharge and SSD for all Siberian rivers, shown in Figure 1 (top).

6. Concluding Remarks

[16] There are several caveats to our analysis. First, we apply the wavelet spectrum analysis only for qualitative comparison: the 30-year salinity time series are not long enough to draw reliable quantitative conclusions from the wavelet analysis. Second, while the residence time of the melt water and river discharge water on the eastern Siberian shelf remains poorly known, we speculate that there is no connection between two consequent summers and/or winters, and the shelf environment does not "remember" the initial hydrographic conditions over a time scale exceeding one year. Third, the ice-related processes were not part of our analysis. We oversimplified our description of winter surface layer by assuming that a one-and-a-half-meter thick layer of sea-ice does not introduce spatial and inter-annual variability. Further detailed analysis of winter salinity and fresh water content variations will help us to address these questions, and is the goal of our future work.

[17] **Acknowledgments.** Financial support through the BMBF project "System Laptev Sea" (03G0639A) is gratefully acknowledged. We thank the International Arctic Research Center at the University of Alaska Fairbanks for additional financial support. SK acknowledges funding through the NAVO grant N00014-04-1-0775 and the BMBF project "Otto-Schmidt-Laboratory for Polar and Marine Sciences" (03PL038A). BT was supported by the Natural Sciences and Engineering Research Council of Canada Discovery Grant Program, and by the National Science Foundation under grant OPP-0230325 from the Office of Polar Programs and grant ARC-05-20496 from the Arctic Science Program. DB acknowledges funds through the DFG grant SP 526/3 and the BMBF 03G0639D project.

References

Aagaard, K., L. K. Coachman, and E. C. Carmack (1981), On the halocline of the Arctic Ocean, *Deep Sea Res.*, *28*, 529–545.

Dmitrenko, I., S. Kirillov, H. Eicken, and N. Markova (2005), Wind-driven summer surface hydrography of the eastern Siberian shelf, *Geophys. Res. Lett.*, *32*, L14613, doi:10.1029/2005GL023022.

Dmitrenko, I. A., S. A. Kirillov, and L. B. Tremblay (2007), The long-term and interannual variability of summer fresh water storage over the eastern Siberian shelf: Implication for climatic change, *J. Geophys. Res.*, doi:10.1029/2007JC004304, in press.

Foufoula-Georgiou, E., and P. Kumar (Eds.) (1995), *Wavelets in Geophysics*, 373 pp., Academic, San Diego, Calif.

Harms, I. H., and M. J. Karcher (1999), Modelling the seasonal variability of circulation and hydrography in the Kara Sea, *J. Geophys. Res.*, *104*(C6), 13,431–13,448.

Johnson, M. A., and I. Polyakov (2001), The Laptev Sea as a source for recent Arctic Ocean salinity change, *Geophys. Res. Lett.*, *28*(10), 2017–2020.

Melling, H., and R. M. Moore (1995), Modification of halocline source waters during freezing on the Beaufort Sea shelf: Evidence from oxygen isotopes and dissolved nutrients, *Cont. Shelf Res.*, *15*(1), 89–113.

Pfirman, S., M. A. Lange, I. Wollenburg, and P. Schlosser (1990), Sea ice characteristics and the role of sediment inclusions in deep-sea deposition Arctic-Antarctic comparisons, in *Geological History of the Polar Oceans Arctic Versus Antarctic*, *NATO ASI Ser., Ser. C*, vol. 308, edited by U. Bleil and J. Thiede, pp. 187–211, Kluwer, Dordrecht, Netherlands.

Polyakov, I. V., and M. A. Johnson (2000), Arctic decadal and interdecadal variability, *Geophys. Res. Lett.*, *27*(24), 4097–4100.

Rothrock, D. A., and J. Zhang (2005), Arctic Ocean sea ice volume: What explains its recent depletion?, *J. Geophys. Res.*, *110*, C01002, doi:10.1029/2004JC002282.

Rudels, B., L. G. Anderson, and E. P. Jones (1996), Formation and evolution of the surface mixed layer and halocline of the Arctic Ocean, *J. Geophys. Res.*, *101*(C4), 8807–8822.

Shpaikher, A. O., and Z. P. Fedorova (1977), Seasonal variability of the heat conditions of the Arctic shelf seas (in Russian), *Proc. Arct. Antarct. Res. Inst.*, *338*, 25–31.

Shpaikher, A. O., and Z. P. Fedorova (1978), Interannual variability of the hydrographic regime over the Siberian shelf seas (in Russian), *Proc. Arct. Antarct. Res. Inst*, *349*, 16–25.

Steele, M., and W. Ermold (2004), Salinity trends on the Siberian shelves, *Geophys. Res. Lett.*, *31*, L24308, doi:10.1029/2004GL021302.

Untersteiner, N. (1968), Natural desalination and equilibrium salinity profile of perennial sea ice, *J. Geophys. Res.*, *73*, 1251–1257.

Walsh, J. E., W. L. Chapman, and T. L. Shy (1996), Recent decrease of sea level pressure in the central Arctic, *J. Clim.*, *9*, 480–486.

D. Bauch and I. A. Dmitrenko, Leibniz Institute of Marine Sciences, University of Kiel, Wichhofstrasse 1–3, D-24105 Kiel, Germany. (idmitrenko@ifm-geomar.de)

S. A. Kirillov and M. Makhotin, Arctic and Antarctic Research Institute, St. Petersburg 199397, Russia.

L. B. Tremblay, Oceans and Atmosphere Sciences, McGill University, 805 Sherbrooke Street West, Montreal, QC, Canada H2A 2K6.